Journal of Molecular Liquids 311 (2020) 113353

Contents lists available at ScienceDirect

Journal of Molecular Liquids

journal homepage: www.elsevier.com/locate/molliq

In-depth investigation on THz spectrum of 1-butyl-3-methylimidazolium dicyanamide spreading on graphene surface by computational calculation

Yongji Guan [a], Jiao Zhang [a], Jinyuan Wang [c], Fulong Yang [d], Huanwang Jing [c], Xiaoping Zhang [a,*], Youquan Deng [b,*]

[a] Institute of Optoelectronics and Electromagnetic Information, School of Information Science and Engineering, Lanzhou University, Lanzhou, 730000, People's Republic of China
[b] Centre for Green Chemistry and Catalysis, Lanzhou Institute of Chemical Physics, Chinese Academy of Sciences, Lanzhou 730000, People's Republic of China
[c] State Key Laboratory of Applied Organic Chemistry, College of Chemistry and Chemical Engineering, Lanzhou University, Lanzhou 730000, People's Republic of China
[d] College of Electrical and Information Engineering, Lanzhou University of Technology, Lanzhou 730050, People's Republic of China

ARTICLE INFO

Article history:
Received 13 March 2020
Received in revised form 30 April 2020
Accepted 10 May 2020
Available online 14 May 2020

ABSTRACT

Understanding dynamic change of ionic liquid (IL) THz spectrum under certain conditions is a real challenge. Herein, through spreading 1-butyl-3-methylimidazolium dicyanamide ([Bmim][DCA]) nanodroplet on graphene surface, dynamic change of [Bmim][DCA] THz spectrum in the range from 30 to 300 cm^{-1} is probed by computational calculation at 300 K. Analyzing the calculated THz spectra it can be found that vibrational bands at 49.95 (cation-anion bend), 216.45 cm^{-1} (rocking of CH_3 in alkyl chain) show a 16.65 cm^{-1} blue shift as spreading time increases from 0 to 5 ns and further blue-shift 16.65 cm^{-1} as spreading time increases from 10 to 20 ns, while vibrational band at 266.40 cm^{-1} (bend of CH_3 in methyl) only blue-shifts 16.65 cm^{-1} as spreading time increases from 0 to 20 ns. The underlying mechanism is revealed to be the stronger adsorbed layer forming on graphene-IL interface which enhances the hydrogen bonds between cations and anions, and constrains the torsion and out-of-plane bend of CH_3 group in alkyl chain and methyl respectively. The findings described here represent an important step in developing a comprehensive understanding of dynamic manipulation IL THz spectrum by spreading IL nanodroplet on graphene surface.

1. Introduction

Terahertz (THz)-frequency infrared spectra contain a wealth of information concerning the structure, intermolecular forces, and dynamics of ionic liquids (ILs) [1,2] and atomistic understanding the dynamic change in the THz spectra of ILs under external conditions is still a challenge. Knowledge of the influence of external conditions on the THz spectra of ILs is very significant for further probing the dynamic change in cohesion energies and intermolecular forces of ILs under certain external conditions because this could help to design and synthesize the "task-specific" ILs [3]. On the other hand, ILs show excellent physicochemical properties which make them attractive as "green" solvents in various fields. Understanding the change of structures and properties of ILs under certain external conditions can promote the further application of ILs-assisted electrochemical synthesis, photo-catalysis, extraction, etc. [4,5]

During the past few decades, the THz spectra of ILs have been investigated from theoretical calculations [6–8] and experimental measurements [2,9–18]. Bhargava and Balasubramanian confirmed that the presence of the hydrogen bond (HB) between the acidic hydrogen in imidazolium ring and the chloride ion in the 1,3-dimethylimidazolium chloride IL influences the C—H stretching mode which results to a red shift the C—H stretching frequency by employing Ab initio molecular dynamics (MD) simulations [6]. Ludwig and coworkers combined the experimental measurements and density functional theory to confirm that the intermolecular stretching modes show blue shift with increasing cation–anion interaction of the ILs due to HBs in the ILs [2,13,14]. Meanwhile, they also reported that shifting of ILs THz frequency stems mainly from varying interaction strength rather than from different reduced masses of the anions [17]. Forsyth et al. employed MD simulations to investigate the interfacial structures of three ILs at a charged and uncharged graphene interface and found that these ILs behave differently both in the bulk phase and near a graphene interface [19]. These previous researches provide the possibility for dynamic manipulation of ILs THz spectrum through spreading IL nanodroplet on graphene surface. However, the very little research known does investigate the dynamic change in the THz spectra of ILs under external conditions, whether experimental measurements or theoretical calculations.

* Corresponding authors.
E-mail addresses: zxp@lzu.edu.cn (X. Zhang), ydeng@licp.cas.cn (Y. Deng).

https://doi.org/10.1016/j.molliq.2020.113353
0167-7322/

To the best our knowledge we present here the first computational calculations of dynamic THz spectra change of 1-butyl-3-methylimidazolium dicyanamide ([Bmim][DCA]) IL nanodroplet spreading on graphene surface in the range from 30 to 300 cm^{-1} at 300 K. The low frequency vibrational bands between 30 and 120 cm^{-1} can be generally assigned to the bending and stretching modes of the cation–anion interaction represented by the $^{+}$C-H···N^{-} HBs in [Bmim][DCA] IL [2]. As spreading time of [Bmim][DCA] IL nanodroplet on graphene surface increases, the frequency shift and intensity change of these bands are consistent with the strength change of the calculated interaction between cations and anions. Thus, we present a dynamic change of the [Bmim][DCA] IL THz spectra through spreading [Bmim][DCA] IL nanodroplet on graphene surface.

2. Computational methods

2.1. Model and method

In this work, the simulation system is comprised of [Bmim][DCA] IL nanodroplet and graphene substrate, as showed in Fig. 1. The radius of [Bmim][DCA] IL nanodroplet is 3.0 nm which includes 340 ions pairs, and the graphene substrate with dimensions of $12.0 \times 15.0\ nm^2$ consists of 7056 carbon atoms. The similar MD simulation method with our previous work [20,21] is employed to probe the dynamic THz spectrum change of [Bmim][DCA] IL nanodroplet on graphene substrate surface. The cations and anions are modeled with the CL&P force field [22–24]. In particular, the total charge of the cations and anions employed here is +0.78e and − 0.78e in order to better characterize the transfer properties of [Bmim][DCA] IL nanodroplet. The system structure of [Bmim][DCA] IL nanodroplet spreading on the graphene surface at spreading times t= 5 ns is showed in Fig. S1. Meanwhile, geometry optimization and frequency calculation of [Bmim][DCA] IL are performed with Gaussian09 [25] at the B3LYP-D3 level in combination with the def2-tzvpd basis set.

2.2. Theory

The vibrational spectra are calculated from MD simulations through employing the Fourier transformation of the velocity autocorrelation function (VACF) of the [Bmim][DCA] IL nanodroplet on the surface of graphene substrate [26–28]. The normal VACF is often defined as.

$$C_v(t) = \frac{\left\langle \vec{v_i}(0)\vec{v_i}(t)\right\rangle}{\left\langle \vec{v_i}(0)\vec{v_i}(0)\right\rangle} \tag{1}$$

where $\vec{v_i}(t)$ represents the velocity of an atom i in a cation or an anion at time t. The angular brackets denote the ensemble average, which is summed over all atoms in a cation or an anion at different initial reference time. The THz vibrational density of states (VDOS) can be calculated routinely by the Fourier cosine transformation of VACF [26–28].

$$S(\omega) = \int_0^{\infty} C_v(t)\ \cos(\omega t)dt \tag{2}$$

If the normal VACF is calculated only from the atoms of cations (or anions), the obtained THz VDOS only includes the characteristic peaks of cations (or anions).

The hydrogen bond formation is defined as the following geometric (distance and angular) criteria

$$\begin{cases} R^{CN} < R_c^{CN} \\ \theta^{NCH} < \theta_c^{NCH} \end{cases} \tag{3}$$

where C is the CR atom of the $[Bmim]^+$ donor and N is the N3A atom of the $[DCA]^-$ acceptor (Fig. 2). R^{CN} is the distance between CR and N3A atoms, while θ^{NCH} is the $^{+}$C-H···N^{-} angle. R_c^{CN} and θ_c^{NCH} are threshold values for the distance and angle of hydrogen bond formation respectively. As reported in previous work, the value for θ_c^{NCH} is often set as 30° [26–29]. The value of R_c^{CN} is obtained from the first minimum of the corresponding radial distribution functions (RDFs) of the bulk [Bmim][DCA] IL at 300 K (Fig. S2).

3. Results and discussion

The THz spectrum of the [Bmim][DCA] IL in the range from 30 to 300 cm^{-1} is presented in Fig. 3 at spreading time t = 0 ns (bulk phase IL) and temperature T = 300 K. As showed in Fig. 3, the THz spectrum of [Bmim][DCA] IL is divided into five main vibrational bands, which can be assigned to the bending mode of the cation-anion bend (49.95 cm^{-1}), the cation-anion stretch (99.90 cm^{-1}), the alkyl chain (Et) torsion (133.20 cm^{-1}), the rocking of CH_3 (Et) in the alkyl chain (216.45 cm^{-1}) and the bend of CH_3 (Methyl, Me) connected to NA atom (266.40 cm^{-1}) [2]. To further understand the contribution of cations and anions to the THz spectrum of [Bmim][DCA] IL, we calculate the THz spectrum of cations $[Bmim]^+$ and anions $[DCA]^-$ respectively and the results are presented in Fig. S3. By comparing these two THz spectra, we found that the intensity of the vibrational bands in cation is significantly stronger than that of the anion. However, for the vibrational band at 49.95 cm^{-1}, the intensity in cation and anion is very close, this indicates that interaction between cation and anion leads to the low frequency vibrational bands.

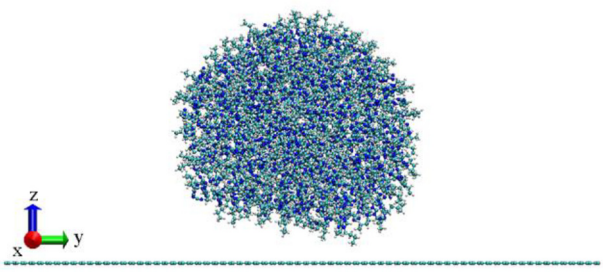

Fig. 1. The computational model comprised of [Bmim][DCA] IL nanodroplet and graphene substrate.

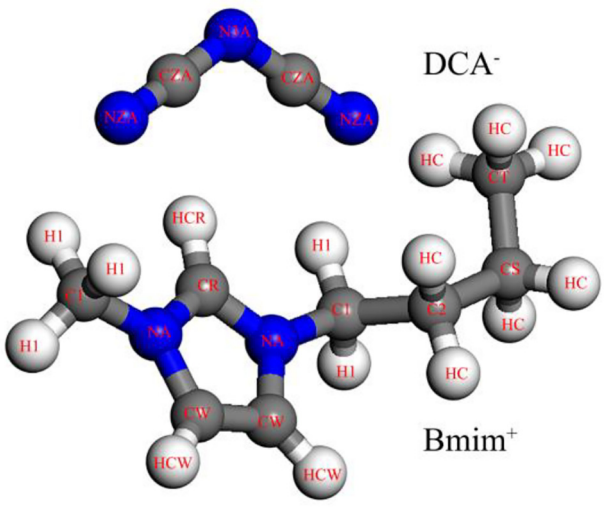

Fig. 2. The molecular structures of 1-butyl-3-methylimidazolium ($[Bmim]^+$) and dicyanamide ($[DCA]^-$).

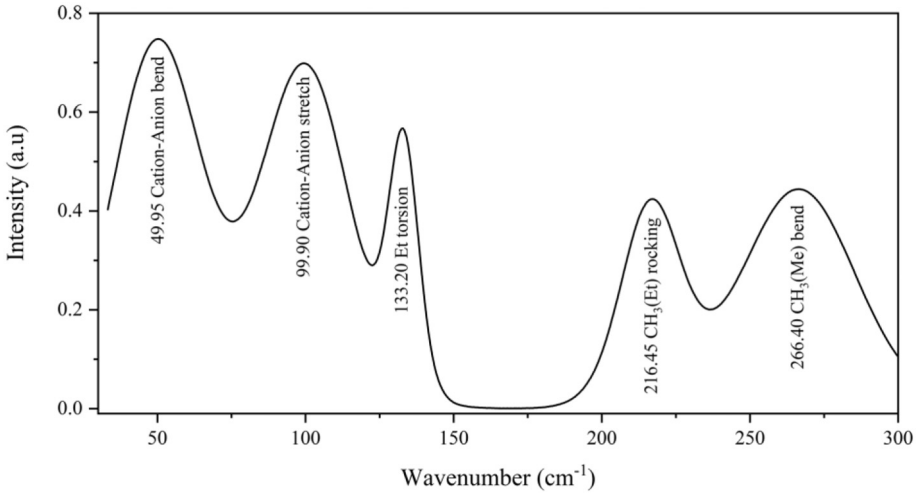

Fig. 3. The THz spectrum of [Bmim][DCA] IL in the range from 30 to 300 cm^{-1} at $t = 0$ ns and T = 300 K.

As [Bmim][DCA] IL nanodroplet gradually spreads along graphene surface, the THz spectra of [Bmim][DCA] IL also change with spreading time. The results are calculated every 5 ns as showed in Fig. 4 and the corresponding vibrational bands are presented in Table S1. As showed in Fig. 4, the maximum value of spreading time is equal to 20 ns, this is because the structure of [Bmim][DCA] IL nanodroplet keeps stable after the spreading time beyond 20 ns, which can be attributed to the balance between internal interaction of [Bmim][DCA] IL and IL-graphene interaction. Our precious work confirmed that a strong adsorbed layer forms at the IL-graphene interface (Fig. S1) when the IL nanodroplet spreads on solid surface [21]. Meanwhile, the structure of the adsorbed layer changes with spreading time of IL nanodroplet on solid surface. Therefore, the strong adsorbed layer makes the spectrum of the IL nanodroplet on solid surface different from the bulk phase and the spectrum also changes with spreading time of IL nanodroplet on solid surface. Through analyzing the THz spectra presented in Fig. 4, we can find the numbers of the vibrational bands are all 5 for spreading time from 0 to 20 ns in the range from 30 to 300 cm^{-1}, but the position of the vibrational bands shifts and the intensity of the vibrational bands changes with spreading time. We can further find the vibrational bands at 49.95, 216.45 and 266.40 cm^{-1} shift to high frequency (blue shift) as the spreading time increases. In order to more clearly show the shift of these three vibrational bands with spreading time, we present the vibrational bands at 49.95, 216.45 and 266.40 cm^{-1} in Fig. 5a, b and c respectively.

As showed in Fig. 5a, the vibrational band at 49.95 cm^{-1} shows a 16.65 cm^{-1} blue shift as spreading time increases from 0 to 5 ns and further blue-shifts 16.65 cm^{-1} as spreading time increases from 10 to 20 ns. Generally, as reported in previous work, a stronger adsorbed layer forms at the solid-liquids interface when the liquids spread on solid surface on the nanoscale [19,21,30,31]. In this work, when the [Bmim][DCA] IL nanodroplet spreads on graphene surface, a stronger adsorbed layer forms near the graphene surface (Fig. S1). Comparing with bulk IL, the adsorbed layer has a nearly doubled density and a rather rigid or solid-like structure. Thus, the stronger adsorbed layer compels more HBs formation between anions and cations which enhances the interaction between cations and anions and makes the vibrational band blue-shift from 49.95 to 66.60 cm^{-1}, further to 83.25 cm^{-1}. As spreading time increases from 0 to 5 ns, the atom numbers in adsorbed layer increases by 20.18% of the total number to ~69. This make the average interaction between IL and graphene substrate reach 17.07 kJ mol^{-1}, and the vibrational band blue-shift 16.65 cm^{-1} compared with 0 ns (bulk phase). It is seen from Fig. 6a that the growth rate of the atom numbers in adsorbed layer decreases but the atom numbers in adsorbed layer is still continually increase with further spreading of [Bmim][DCA] IL nanodroplet on graphene surface.

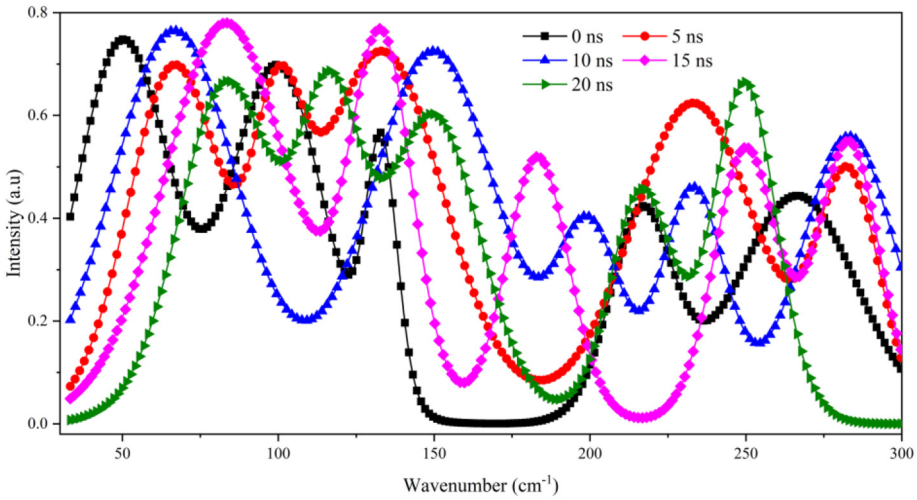

Fig. 4. The THz spectrum of [Bmim][DCA] IL in the range from 30 to 300 cm^{-1} at T = 300 K under different spreading time.

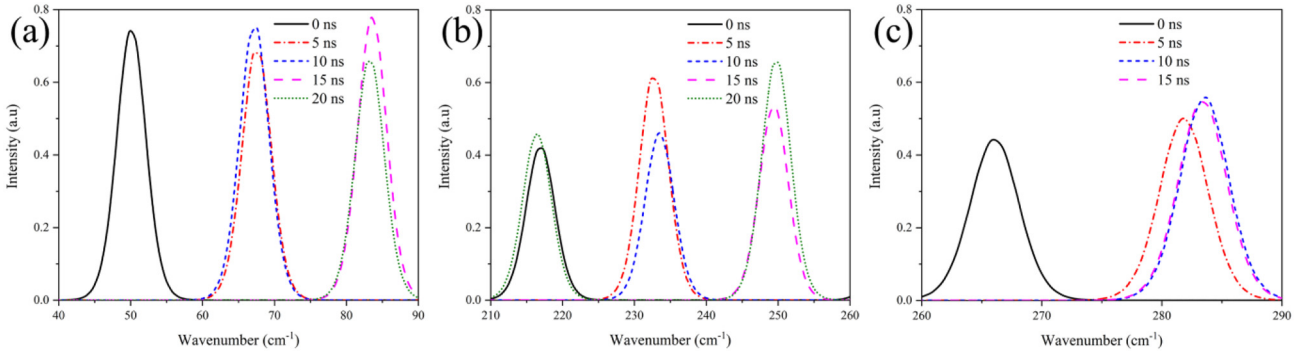

Fig. 5. The vibrational bands of [Bmim][DCA] IL at (a) 49.95, (b) 216.45 and (c) 266.40 cm^{-1} at 300 K under different spreading time.

Therefore, the interaction between IL and graphene substrate is further enhanced (Fig. 6b). When the spreading time increases to 15 ns, the enhanced IL-graphene interaction (Fig. 6b) makes the atom numbers in adsorbed layer increase to 29% of the total number (Fig. 6a) and the numbers of the average HBs between cations and anions further increase by 8.10% to 2.54 (Fig. 6c). More HBs between cations and anions leads to stronger interaction between cations and anions which makes the vibrational band further shift from 66.60 to 83.25 cm^{-1}.

In the case of the vibrational band at 216.45 cm^{-1} which is assigned the rocking of CH_3 (Et) in the alkyl chain. As showed in Fig. 5b, likewise, the vibrational band shows a 16.65 cm^{-1} blue shift as spreading time increases from 0 to 5 ns and further blue-shifts 16.65 cm^{-1} as spreading time increases from 10 to 20 ns. As the [Bmim][DCA] IL nanodroplet gradually spreads on the surface of the graphene substrate, more cations and anions are accumulated in the adsorbed layer (Fig. 6a). However, due to the different average interaction between the graphene substrate and per cation and anion (Fig. 7a), the numbers of cations and anions in the adsorbed layer are not the same (Fig. 7b). Fig. 7b clearly indicates that the numbers of anions in the adsorbed layer are significantly higher than the numbers of cations, which means that the number of cations in the bulk phase of the IL nanodroplet is greater than that of the anions. Thus the excess cations in the bulk phase of IL nanodroplet are less constrained, the CH_3 (Et) rocking is enhanced and then results in the CH_3 (Et) rocking mode displaying a blue-shift, and the blue-shift further increases as the numbers of cations in bulk phase of the IL nanodroplet increase. On the other hand, as the IL nanodroplet continues to spread the surface of the graphene substrate, the area of the gas-IL interface increases. It is well known that the alkyl chains in ILs are usually concentrated at the gas-ILs interface [32]. A larger gas-liquid interface means that more alkyl chains at the interface, which leads to more free rocking of CH_3 (Et) and also makes the CH_3 (Et) rocking mode shift to high frequency. It is worth noting that a relatively weak vibrational band appears at 216.45 cm^{-1} as spreading time increase to 20 ns. Through analyzing the vibrational bands of cations and anions at different spreading time (Fig. S3 and S4), we find that the anion bend at 183.15 cm^{-1} shows a 16.65 cm^{-1} blue shift as spreading time increases from 0 to 15 ns and further blue-shifts 16.65 cm^{-1} as spreading time increases to 20 ns. As mentioned above, the intensity of the vibrational bands in cation is generally stronger than that of the anion, but the intensity of the vibrational band in cation is relatively weaker and it is stronger in anion at 20 ns. Thus, the vibrational band of the anion and cation superpose each other to make a weaker vibrational band appear at 216.45 cm^{-1}.

For the vibrational band at 266.40 cm^{-1} which can be assigned the bend of CH_3 (Me) connected to NA atom. As showed in Fig. 7a, the interaction between graphene and per cation increases with the increasing of spreading time, thus makes the imidazolium ring of the cation lie more horizontally on the graphene surface [21,32]. This is quantified through the second-order Legendre polynomials $P_2(\cos(\theta)) = (3\cos^2(\theta) - 1)/2$, where θ is the calculated angle between the vector perpendicular to the graphene substrate (z axis) and selected vectors (CR-CW, Fig. 2) in cations in the adsorbed layer. The calculated results are plotted in Fig. 8. The horizontal structure of imidazolium ring on the graphene surface constrains the out-of-plane bend of CH_3 (Me) and weakens the strength of the vibrational band. On the other hand, due to the numbers of cations are more than the anions in bulk phase IL, the excess cations in the bulk phase of IL nanodroplet are obtained more free space and then enhances the out-of-plane bend of CH_3 (Me) which make the vibrational band at 266.40 cm^{-1} shift towards the high frequency 283.05 cm^{-1}. However, when the [Bmim][DCA] IL nanodroplet completely spreads the surface of the graphene substrate ($t = 20$ ns), that is, when the contact angle of [Bmim][DCA] IL nanodroplet on graphene surface reaches saturation, the [Bmim][DCA] IL nanodroplet become an approximate IL film. At this time, the limiting effect of the cations and anions in the adsorbed layer on the cations and anions in the bulk phase is further enhanced which significantly constrains the out-of-plane bend of CH_3 (Me), and thus the out-of-plane bend of CH_3 (Me) is very weakened or even disappeared.

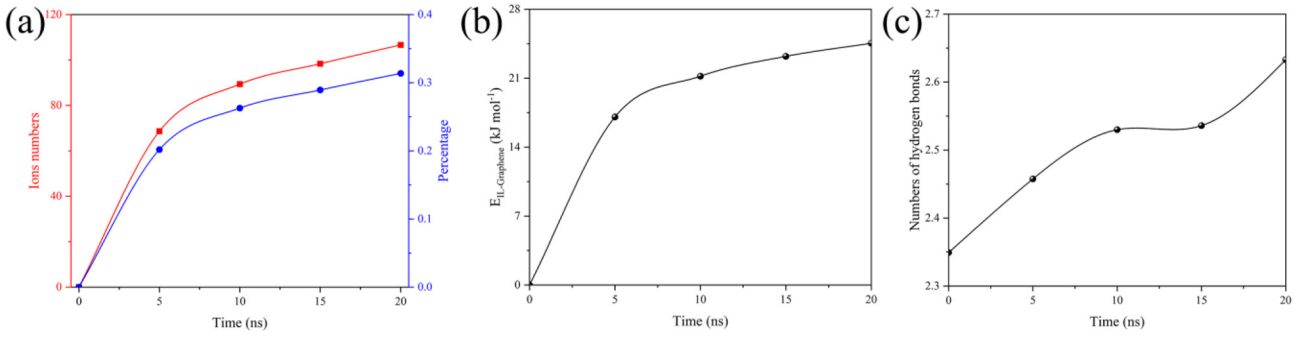

Fig. 6. The ions numbers in adsorbed layer and the proportion of the adsorbed layer ions accounting for the total ion pairs of the IL nanodroplet at (a), the average interaction between IL and graphene at (b) and the average numbers of HBs per cation at (c) as a function of spreading time at 300 K.

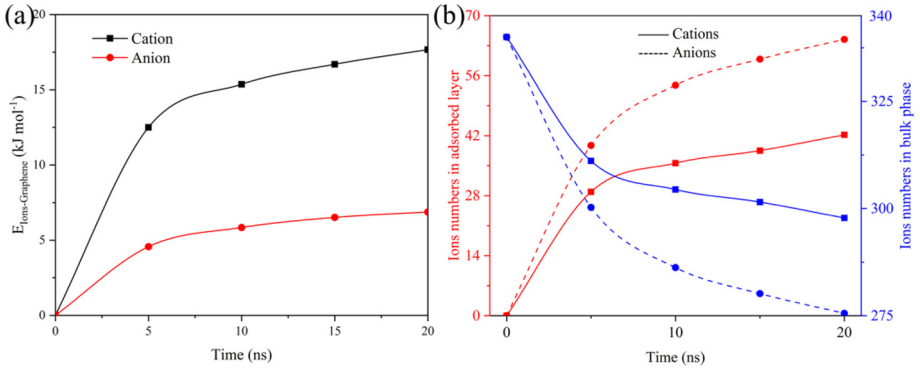

Fig. 7. The average interaction between graphene and per cation and anion at (a) and the cations and anions numbers in adsorbed layer and bulk phase of the IL nanodroplet at (b) as a function of spreading time at 300 K.

4. Conclusions

In summary, computational calculations including MD simulations and density functional theory are employed to investigate the dynamic THz spectra of [Bmim][DCA] IL in the range from 30 to 300 cm^{-1} at 300 K by spreading [Bmim][DCA] IL nanodroplet on graphene surface. According to simulation results, it is seen that the cations and anions are responsive to the THz spectra of [Bmim][DCA] IL nanodroplet on graphene surface and change of cations and anions structures have effect on the THz spectra. When the spreading time of [Bmim][DCA] IL nanodroplet on graphene surface increases, the structures of cations and anions in bulk phase and near graphene surface change. Thus, the vibrational bands shift as spreading time increases. Further analysis indicates that the vibrational bands at 49.95, 216.45 cm^{-1} show a 16.65 cm^{-1} blue shift as spreading time increases from 0 to 5 ns and further blue-shift 16.65 cm^{-1} as spreading time increases from 10 to 20 ns, while the vibrational band at 266.40 cm^{-1} only blue-shifts 16.65 cm^{-1} as spreading time increases from 0 to 20 ns. These results can be mainly attributed to the stronger adsorbed layer forming on the graphene-IL interface and changes the structures of cations and anions near graphene surface which further changes the dynamic behavior of cations and anions in bulk phase. Due to the enhancement of the HBs between cations and anions as spreading time increases, the vibrational band at 49.95 cm^{-1} shows a 16.65 cm^{-1} blue shift from 0 to 5 ns and further blue-shift 16.65 cm^{-1} from 10 to 20 ns. For the vibrational bands at 216.45 cm^{-1}, the strong adsorbed layer constraints the rocking of CH_3 (Et) in the alkyl chain and make the vibrational band shift to high frequency about 16.65 cm^{-1} from 0 to 5 ns and further shift 16.65 cm^{-1} from 10 to 20 ns. The vibrational band at 266.40 cm^{-1} assigned the bend of CH_3 (Me) connected to NA atom shows a blue-shift of 16.65 cm^{-1} as spreading time increases from 0 to 15 ns which is caused by constraining of the strong adsorbed layer on the out-of-plane bend of CH_3 (Me). When the [Bmim][DCA] IL nanodroplet become an approximate IL film on graphene surface, the out-of-plane bend of CH_3 (Me) is further constrained and the vibrational band is very weakened or even disappeared. This work thus do provide an innovative perspective on the dynamical manipulation of [Bmim][DCA] IL THz spectrum through spreading IL nanodroplet on the graphene surface.

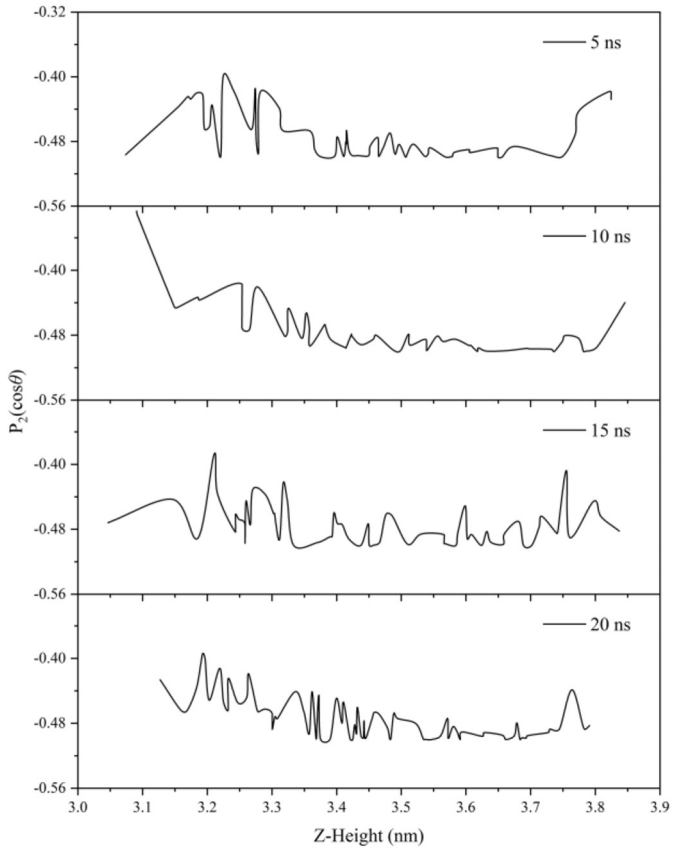

Fig. 8. The average $P_2(\cos\theta)$ for the angles between the selected vectors (CR-CW) and the graphene substrate normal (z axis) in the adsorbed layer from 5 to 20 ns at 300 K.

CRediT authorship contribution statement

Yongji Guan: Conceptualization, Data curation, Formal analysis, Funding acquisition, Investigation, Methodology, Software, Visualization, Writing - original draft, Writing - review & editing. **Jiao Zhang:** Data curation, Methodology, Software. **Jinyuan Wang:** Investigation, Methodology, Software, Visualization. **Fulong Yang:** Visualization. **Huanwang Jing:** Software. **Xiaoping Zhang:** Conceptualization, Funding acquisition, Project administration, Supervision. **Youquan Deng:** Conceptualization, Funding acquisition, Project administration, Supervision.

Declaration of competing interest

The authors declare that they have no known competing financial interests or personal relationships that could have appeared to influence the work reported in this paper.

Acknowledgments

The authors acknowledge the financial support of this work from the Lanzhou University International Teacher Postdoctoral Scholarship Fund, the National Key Research and Development Program of China

(2017YFA0403101), the Fundamental Research Funds for the Central Universities (lzujbky-2018-it62 and lzujbky-2018-127) and the National Natural Science Foundation of China (61804071).

Appendix A. Supplementary data

See the supplementary material for the system structure of [Bmim][DCA] IL spreading on the graphene surface at $t = 5$ ns and T = 300 K; the radical distribution function (RDF) between the CR ($[Bmim]^+$) and N3A ($[DCA]^-$) atoms for the bulk [Bmim][DCA] IL at T = 300 K; the THz spectrum of cations $[Bmim]^+$ and anions $[DCA]^-$ in the range from 30 to 300 cm^{-1} at $t = 0$ ns and T = 300 K; the vibrational bands of [Bmim][DCA] IL THz spectra in the range from 30 to 300 cm^{-1} at T = 300 K under different spreading time; the THz spectra of cations and anions in the range from 30 to 300 cm^{-1} at 300 K under different spreading time, (a) $t = 5$ ns, (b) $t = 10$ ns, (c) $t = 15$ ns, (d) $t = 20$ ns. Supplementary data to this article can be found online at doi:https://doi.org/10.1016/j.molliq.2020.113353.

References

[1] V.H. Paschoal, L.F.O. Faria, M.C.C. Ribeiro, Vibrational spectroscopy of ionic liquids, Chem. Rev. 117 (2017) 7053.
[2] K. Fumino, A. Wulf, R. Ludwig, The cation–anion interaction in ionic liquids probed by far-infrared spectroscopy, Angew. Chem. Int. Ed. 47 (2008) 3830.
[3] S. Zhang, J. Zhang, Y. Zhang, Y. Deng, Nanoconfined ionic liquids, Chem. Rev. 117 (2017) 6755.
[4] J. Di, J. Xia, Y. Ge, L. Xu, H. Xu, M. He, Q. Zhang, H. Li, Reactable ionic liquid-assisted rapid synthesis of BiOI hollow microspheres at room temperature with enhanced photocatalytic activity, J. Mater. Chem. A 2 (2014) 15864.
[5] T. Chatzimitakos, C. Binellas, K. Maidatsi, C. Stalikas, Magnetic ionic liquid in stirring-assisted drop-breakup microextraction: proof-of-concept extraction of phenolic endocrine disrupters and acidic pharmaceuticals, Anal. Chim. Acta 910 (2016) 53.
[6] B.L. Bhargava, S. Balasubramanian, Intermolecular structure and dynamics in an ionic liquid: a Car–Parrinello molecular dynamics simulation study of 1,3-dimethylimidazolium chloride, Chem. Phys. Lett. 417 (2006) 486.
[7] S.A. Katsyuba, E.E. Zvereva, A. Vidiš, P.J. Dyson, Application of density functional theory and vibrational spectroscopy toward the rational design of ionic liquids, J. Phys. Chem. A 111 (2007) 352.
[8] S.S. Sarangi, S.K. Reddy, S. Balasubramanian, Low frequency vibrational modes of room temperature ionic liquids, J. Phys. Chem. B 115 (2011) 1874.
[9] A. Dominguez-Vidal, N. Kaun, M.J. Ayora-Cañada, B. Lendl, Probing intermolecular interactions in water/ionic liquid mixtures by far-infrared spectroscopy, J. Phys. Chem. B 111 (2007) 4446.
[10] K. Fumino, A. Wulf, R. Ludwig, The potential role of hydrogen bonding in aprotic and protic ionic liquids, Phys. Chem. Chem. Phys. 11 (2009) 8790.
[11] T. Köddermann, K. Fumino, R. Ludwig, J.N. Canongia Lopes, A.A.H. Pádua, What far-infrared spectra can contribute to the development of force fields for ionic liquids used in molecular dynamics simulations, ChemPhysChem 10 (2009) 1181.
[12] T. Buffeteau, J. Grondin, Y. Danten, J.-C. Lassègues, Imidazolium-based ionic liquids: quantitative aspects in the far-infrared region, J. Phys. Chem. B 114 (2010) 7587.
[13] C. Roth, T. Peppel, K. Fumino, M. Köckerling, R. Ludwig, The importance of hydrogen bonds for the structure of ionic liquids: single-crystal X-ray diffraction and transmission and attenuated total reflection spectroscopy in the terahertz region, Angew. Chem. Int. Ed. 49 (2010) 10221.
[14] A. Wulf, K. Fumino, R. Ludwig, Spectroscopic evidence for an enhanced anion–cation interaction from hydrogen bonding in pure imidazolium ionic liquids, Angew. Chem. Int. Ed. 49 (2009) 449.
[15] A. Wulf, K. Fumino, R. Ludwig, P.F. Taday, Combined THz, FIR and Raman spectroscopy studies of Imidazolium-based ionic liquids covering the frequency range 2–300 cm^{-1}, ChemPhysChem 11 (2010) 349.
[16] K. Fumino, E. Reichert, K. Wittler, R. Hempelmann, R. Ludwig, Low-frequency vibrational modes of protic molten salts and ionic liquids: detecting and quantifying hydrogen bonds, Angew. Chem. Int. Ed. 51 (2012) 6236.
[17] K. Fumino, K. Wittler, R. Ludwig, The anion dependence of the interaction strength between ions in imidazolium-based ionic liquids probed by far-infrared spectroscopy, J. Phys. Chem. B 116 (2012) 9507.
[18] K. Fumino, V. Fossog, P. Stange, K. Wittler, W. Polet, R. Hempelmann, R. Ludwig, Ion pairing in protic ionic liquids probed by far-infrared spectroscopy: effects of solvent polarity and temperature, ChemPhysChem 15 (2014) 2604.
[19] S. Begić, E. Jónsson, F. Chen, M. Forsyth, Molecular dynamics simulations of pyrrolidinium and imidazolium ionic liquids at graphene interfaces, Phys. Chem. Chem. Phys. 19 (2017) 30010.
[20] Y. Guan, Q. Shao, W. Chen, J. Zhang, X. Zhang, Y. Deng, Flow-induced voltage generation by driving imidazolium-based ionic liquids over a graphene nano-channel, J. Mater. Chem. A 6 (2018) 11941.
[21] Y. Guan, Q. Shao, W. Chen, S. Liu, X. Zhang, Y. Deng, Dynamic three-dimensional nanowetting behavior of imidazolium-based ionic liquids probed by molecular dynamics simulation, J. Phys. Chem. C 121 (2017) 23716.
[22] J.N. Canongia Lopes, A.A.H. Pádua, Molecular force field for ionic liquids III: imidazolium, pyridinium, and phosphonium cations; chloride, bromide, and dicyanamide anions, J. Phys. Chem. B 110 (2006) 19586.
[23] J.N. Canongia Lopes, J. Deschamps, A.A.H. Pádua, Modeling ionic liquids using a systematic all-atom force field, J. Phys. Chem. B 108 (2004) 11250.
[24] J.N. Canongia Lopes, J. Deschamps, A.A.H. Pádua, Modeling ionic liquids using a systematic all-atom force field, J. Phys. Chem. B 108 (2004) 2038.
[25] M.J. Frisch, G.W. Trucks, H.B. Schlegel, G.E. Scuseria, M.A. Robb, J.R. Cheeseman, G. Scalmani, V. Barone, G.A. Petersson, H. Nakatsuji, X. Li, M. Caricato, A. Marenich, J. Bloino, B.G. Janesko, R. Gomperts, B. Mennucci, H.P. Hratchian, J.V. Ortiz, A.F. Izmaylov, J.L. Sonnenberg, D. Williams-Young, F. Ding, F. Lipparini, F. Egidi, J. Goings, B. Peng, A. Petrone, T. Henderson, D. Ranasinghe, V.G. Zakrzewski, J. Gao, N. Rega, G. Zheng, W. Liang, M. Hada, M. Ehara, K. Toyota, R. Fukuda, J. Hasegawa, M. Ishida, T. Nakajima, Y. Honda, O. Kitao, H. Nakai, T. Vreven, K. Throssell, J.J.A. Montgomery, J.E. Peralta, F. Ogliaro, M. Bearpark, J.J. Heyd, E. Brothers, K.N. Kudin, V.N. Staroverov, T. Keith, R. Kobayashi, J. Normand, K. Raghavachari, A. Rendell, J.C. Burant, S.S. Iyengar, J. Tomasi, M. Cossi, J.M. Millam, M. Klene, C. Adamo, R. Cammi, J.W. Ochterski, R.L. Martin, K. Morokuma, O. Farkas, J.B. Foresman, D.J. Fox, Gaussian 09 Rev. A.02, Gaussian Inc, Wallingford, CT, 2009.
[26] Z. Dai, L. Shi, L. Lu, Y. Sun, X. Lu, Unique structures and vibrational spectra of protic ionic liquids confined in TiO_2 slits: the role of interfacial hydrogen bonds, Langmuir 34 (2018) 13449.
[27] G. Zhou, Y. Li, Z. Yang, F. Fu, Y. Huang, Z. Wan, L. Li, X. Chen, N. Hu, L. Huang, Structural properties and vibrational spectra of ethylammonium nitrate ionic liquid confined in single-walled carbon nanotubes, J. Phys. Chem. C 120 (2016) 5033.
[28] G. Zhou, Z. Yang, F. Fu, Y. Huang, X. Chen, Z. Lu, N. Hu, Molecular-level understanding of solvation structures and vibrational spectra of an ethylammonium nitrate ionic liquid around single-walled carbon nanotubes, Ind. Eng. Chem. Res. 54 (2015) 8166.
[29] R. Kumar, J.R. Schmidt, J.L. Skinner, Hydrogen bonding definitions and dynamics in liquid water, J. Chem. Phys. 126 (2007) 204107.
[30] C. Herrera, G. García, M. Atilhan, S. Aparicio, Nanowetting of graphene by ionic liquid droplets, J. Phys. Chem. C 119 (2015) 24529.
[31] Y.-L. Wang, Z.-Y. Lu, A. Laaksonen, Heterogeneous dynamics of ionic liquids in confined films with varied film thickness, Phys. Chem. Chem. Phys. 16 (2014) 20731.
[32] M. Atilhan, S. Aparicio, Theoretical study of low viscous ionic liquids at the graphene interface, J. Phys. Chem. C 122 (2018) 1645.